Building and Environment 248 (2024) 111098

Contents lists available at ScienceDirect

Building and Environment

journal homepage: www.elsevier.com/locate/buildenv

A data-driven model on human thermophysiological and psychological responses under dynamic solar radiation

Yuchen Ji, Jusheng Song, Pengyuan Shen *

School of Architecture, Harbin Institute of Technology, Shenzhen, 518055, China

A B S T R A C T

Excessive solar radiation can also cause thermophysiological and psychological discomfort in the human body. In real-world environments, solar radiation is highly variable. Moreover, the amount of solar radiation exposure that people receive due to their outdoor activities can have large fluctuation. The physiological and psychological responses of the human body under this dynamic solar radiation exposure are quite different from those under steady-state solar radiation exposure. Therefore, this paper studies the physiological and psychological responses of the human body under the condition of dynamic solar radiation through the method of field experimental research and explores the applicability of the existing indicators of PET and UTCI in the dynamic radiation environment. A novel recurrent neural network model was used to predict skin temperatures and thermal sensations, in which genetic algorithm was applied to tune hyper-parameters.

It is noteworthy that both thermal sensations and skin temperatures at exposed body segments show a stronger correlation to solar radiation, while there exists a time lag between solar radiation and skin temperature when people are exposed to solar radiation. Compared with thermophysiological models (DTS), the GA-LSTM model has a better prediction accuracy in thermal sensations.

1. Introduction

The World Meteorological Organization (WMO) Statement on the State of the Global Climate in 2019 released by the United Nations emphasizes that climate change continues to affect human social and economic development, health, and food security [1], as well as energy consumption [2]. Unprecedented high temperatures in Australia, India, Japan, and Europe adversely affected health and well-being, resulting in more than 100 deaths in Japan due to the extremely hot weather [1]. Urban environment is more susceptible to overheating due to the combined impact of climate change and urban heat island (UHI) [3–5]. Urban areas are more vulnerable and influenced by UHI and population density [6]. A synergic effect of heat waves and UHI could cause impressive health and discomfort problems [7]. Solar radiation is an important cause of high temperature and directly affects outdoor thermal comfort. A moderate amount of solar radiation, such as ultraviolet B (UVB), is beneficial to human health as it promotes the production of vitamin D for bone health [8]. However, excessive solar UV radiation exposure can lead to short-term skin reactions (erythema) and long-term skin illness (skin cancer) [8–10]. In addition to UV damage, visible and infrared light can also cause skin damage like sunburn, or even toxic photochemical reactions in the skin [11]. The ultimate exposure time decreases significantly with increasing irradiation intensity [12,13]. An exponential relationship between the effective insult temperature and the time of exposure in determining the burn severity was revealed as shown in Equation (1) [14]:

$$t = t_b \exp\left(T_b - T\right) \tag{1}$$

where t is limited time of exposure, s, t_b is basal time of exposure, s, T_b is basal effective insult temperature, °C, T is effective insult temperature, °C.

Excessive solar radiation not only poses health risks but also causes physiological and psychological discomfort in individuals in both indoor [15] and outdoor environment [16]. Therefore, it is crucial to pay attention to the influence of solar radiation on human thermal comfort.

1.1. Outdoor thermal comfort studies

Outdoor thermal exposures on humans can vary due to climate, weather conditions, seasons, vegetation, and surroundings, as well as personnel activities. Thus, outdoor thermal comfort is a dynamic process. Solar radiation and wind speed are the most uncertain among the factors influencing outdoor thermal environments. An experiment conducted in Hong Kong focused on the influence of solar radiation and wind speed on outdoor thermal comfort [17]. Humans might be more sensitive to changes in solar radiation than the predicted model. Besides, in summer, solar radiation influences thermal comfort significantly, which can be adjustable through the arrangement of buildings and

* Corresponding author.School of Architecture, Harbin Institute of Technology Shenzhen, China
E-mail address: shenpengyuan@hit.edu.cn (P. Shen).

https://doi.org/10.1016/j.buildenv.2023.111098
Received 11 September 2023; Received in revised form 22 November 2023; Accepted 1 December 2023
Available online 6 December 2023

greenery. Numerous studies have been conducted in similar climate zones, focusing on summer overheating issues [18–20]. An interesting finding is that when the Universal Thermal Climate Index (UTCI) exceeds 26 °C, solar radiation would take a dominant role in outdoor thermal comfort rather than wind speed [21].

In addition to climate influences, living habits and cultural backgrounds may also affect human thermal responses to the outdoor thermal environment. A comparison on the human thermal responses in Hong Kong and Melbourne in summer was conducted, which found that the thermal neutral temperature differs a lot for residents in these two areas [22].

Numerous outdoor thermal comfort studies considering the effects of solar radiation were conducted across the world, covering different climate conditions. In these studies, the most commonly used indexes for evaluating outdoor thermal comfort are Mean Radiant Temperature (MRT), UTCI, Physiological Equivalent Temperature (PET), and operative temperature. A linear regression model was mostly established to describe the relationship between thermal sensations and a universal environmental index. Consequently, we can hardly acquire thermal comfort and thermal adaptations changes with time from these models.

1.2. Dynamic thermal comfort based on physiology and psychology

Human thermal sensation is a reflection of neural activities generated by the nerve endings, which function as thermal receptors. When the surrounding environment changes, the nerve endings will receive the stimuli and transfer the signal to the brain. Then the brain will make a decision on hot/cold feeling and give feedback to nerve regulation system. The heat transfer between the human body and thermal environment and nerve signal transfer are the physiological basis of human thermal sensation. Therefore, to completely understand the human thermal sensation mechanism, we should integrate thermal physiological and psychological responses to thermal environments.

The human thermophysiological model based on the human heat equilibrium equation and heat transfer theory is the primary tool to figure out the thermophysiological state of the human body [23–25]. Thermophysiological parameters (skin temperature, core temperature) of the human body can be obtained through the thermophysiological model, which then can be used to determine the thermal comfort. For example, in Gagge's two-node model, the thermophysiological model of the human body consists of passive and active systems. In the passive system, the human body is simplified as a cylinder of two concentric layers (core layer and skin layer). The heat transfer process consists of two parts: heat transfer between the environment and the skin, and heat transfer between the core and the skin. In active systems, four types of regulation, i.e., vasoconstriction, vasodilation, shivering, and sweating, are typically considered, which can be quantitatively described by some linear regulation models using the temperature difference between the skin or core temperature and the reference temperature as the input signal [23].

When the air temperature changes abruptly, psychological responses such as thermal sensations precede thermophysiological responses (skin temperature), especially when the air temperature drops sharply. When the air temperature rises suddenly, the increase in skin temperature is minimal, and it reaches stability quickly due to rapid thermoregulation, while the opposite is true when the temperature drops sharply [26]. Zhang et al. confirmed the phenomenon of psychological advance through experimental research, and established a binomial relationship between thermal sensation and skin temperature [27]. The occurrence of physiological lag or psychological advance may be attributed to physiological regulation. The weaker the physiological regulation, the more noticeable the physiological lag becomes. In addition, there are heat waves and oscillations in the heat transfer process of the human body in the dynamic radiation environment, which deviates from the Fourier heat transfer theory [28,29]. Therefore, to evaluate thermal comfort under dynamic thermal environments, there may exist a temporal bias if only considering skin temperature as a dynamic input.

In addition to skin/core temperatures, human thermal load, as a thermophysiological index, has also been applied to evaluate outdoor thermal comfort under steady and unsteady conditions [30]. Similarly, a relationship between human-body exergy and thermal sensation was explored in unsteady states [31]. Furthermore, based on the dynamic two-node IMEM model [32], human thermophysiological parameters were simulated under unsteady conditions. Human thermophysiolgical and thermal sensation responses were analyzed under rapid and simultaneous solar and wind exposures [33]. Thermal psychological responses were investigated under step-change phases in outdoor environments [34].

The frequency of changes in the dynamic environment should be lower than the frequency of changes in human physiology or psychology. From the above research, it can be seen that when the ambient temperature suddenly changes, the thermal sensations respond rapidly. In the first 2 min of a sudden ambient temperature change, the thermal sensation transcendence is the most obvious, while there was a delay of several minutes for physiological parameters (skin temperature and core temperature) [29]. For solar radiation, the amount of surface solar radiation basically does not change on a minute scale. However, due to the relative movement between people's activities, buildings and greenery, the human body's exposure to solar radiation on the minute scale can vary considerably Therefore, the physiological and psychological responses of the human body under this dynamic solar radiation exposure are quite different from those under steady-state solar radiation exposure.

For thermal psychological evaluation, on-site subjective evaluation and predictive thermal comfort model are two common methods to access thermal response on the environment. The on-site evaluation involves obtaining the evaluation on thermal environment through subjective questionnaires. Common indicators include thermal sensation vote (TSV), thermal comfort vote (TCV), and thermal acceptability vote (TAV), and etc. The predictive thermal comfort model refers to a regression relationship between the thermal comfort evaluation index and the environmental parameters, and the predicted human thermal comfort evaluation can be obtained according to the fitting model when the environmental parameters are measured. For example, Fanger's Predicted Mean Vote and Predicted Percentage of the Dissatisfied (PMV-PPD) is the most widely-used predictive thermal comfort model for steady-state conditions [35], in which the inputs include air temperature, mean radiation temperature, air velocity, relative humidity, clothing insulation, and personnel activity level. However, numerous field studies indicates that there exists a bias when applying PMV model in predicting thermal sensation in real environments, especially in naturally ventilated buildings or buildings where people have adjustments [36,37]. In a dynamic environment, there exists a time lag of human thermal physiological responses or an advance of psychological responses [38]. Therefore, for dynamic thermal environments, especially for dynamic solar radiation exposures, traditional thermal sensation prediction models cannot account for additional thermal sensation changes due to dynamic temporal changes. Factors of thermal environment, thermophysiology and adaptation may be integrated to develop a comprehensive dynamic thermal comfort model [39].

1.3. Thermal comfort indicators

At present, the evaluation of the impact of solar radiation on human comfort primarily relies on steady-state models. Based on these models, PMV, Effective Temperature (ET*), Standardized Effective Temperature (SET), UTCI, and PET are widely used to evaluate human thermal comfort. In Fanger's PMV model [35], the radiation term only accounts for long-wave radiation heat transfer between humans and the surrounding environment, neglecting the effects of solar radiation. The current indoor environmental evaluation standards worldwide are mainly based on the PMV-PPD model, so these standards cannot predict

Table 1
Demographic information.

	Age	Height (cm)	Weight (kg)	BMI (kg/m2)
Max	27	179	80	28.7
Min	19	158	45	17.3
Mean	23.9	167.5	58.1	20.68
Std. Dev.	1.69	5.91	10.01	3.33

thermal comfort status well under solar radiation conditions.

To overcome the gap of solar radiation, La Gennusa et al. proposed a comprehensive method to calculate MRT in indoor thermal environment under the condition of solar radiation. Their approach involves distinguishing between direct irradiation and diffuse solar radiation and integrating it with environmental radiation heat exchange The developed calculation formula for MRT is given in Equation (2) [40]:

$$\overline{T}_{r,irr} = \sqrt[4]{\sum_{i=1}^{N} F_{s\rightarrow i} T_i^4 + \frac{C_{dn}}{\varepsilon \sigma}\left(\alpha_{irr,d} \sum^{M} F_{s\rightarrow i} I_{d,j}^{in} + C_s^{in} \alpha_{irr,d} f_p I_{bn}^{in}\right)} \tag{2}$$

By incorporating the calculated MRT affected by solar radiation into the PMV formula, it is possible to correct the original model that did not consider the influence of solar radiation. Similarly, Zhang et al. also revised the PMV and proposed the CPMV index to evaluate the indoor thermal comfort under the condition of solar radiation. In addition, the author also proposed a formula for calculating the operating temperature considering solar radiation [41].

However, PMV model is just enforceable in steady conditions. For transient conditions, Fiala developed a dynamic thermal sensation model (DTS), which is derived from a relationship between time series of TSV from experiments with dynamic physiological parameters predicted by Fiala multi-node thermoregulation model [42]. The regression analysis considered the nonlinear trend of measured sensation votes when TSV approaches asymptotically the lower and upper limit of the ASHRAE 7-point scale. This was accomplished by using the function of tanh in the regressions. This model predicts dynamic thermal sensation well and can account for the adaptive thermal behavior effects. Similarly, dynamic models for local and overall thermal sensations in Zhang's model were put forward taking first derivative of the skin/core temperature into account [43]. de Dear introduced a dynamic indicator to represent thermal response in transient environments. This model relates this dynamic index with heat flux through the skin and first derivative of skin temperature [44], which are exploited and validated in transient conditions by Zolfaghari and Maerefat [45,46].

ET* and SET are two indicators proposed by Gagge to evaluate the thermal environment based on the heat balance equation [23,47]. SET is derived from ET* but takes into account the influence of activity level and clothing thermal resistance. It is defined as an effective temperature experienced by a person wearing standard clothing under specific conditions, including 50 % relative humidity and no air velocity, and air temperature equal to MRT. In a uniform environment, if the average skin temperature and skin wetness of a person under actual environmental conditions are the same as those under a temperature, the temperature is SET corresponding to the actual environment. This indicator offers the advantage of standardizing the thermal insulation of personnel clothing, so as to better compare the thermal sensation of the human body. Similar to the PMV model, ET* and SET do not take into account the solar radiation well, so they need to be corrected before they can be used for thermal comfort evaluation in a solar radiation environment.

In this paper, we focused on dynamic thermal comfort under step-change solar radiation exposures. The variation characteristics of thermal psychological and physiological responses were analyzed to excavate time discrepancy between human responses and thermal environment parameters. A novel recurrent neural network model was used to predict skin temperatures and thermal sensations, in which

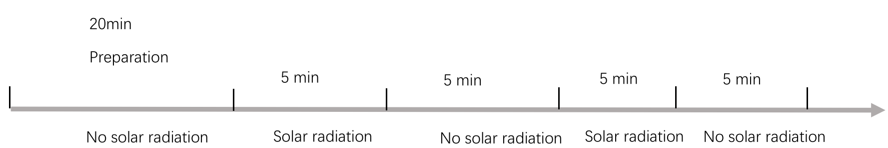

Fig. 1. Experiment procedure.

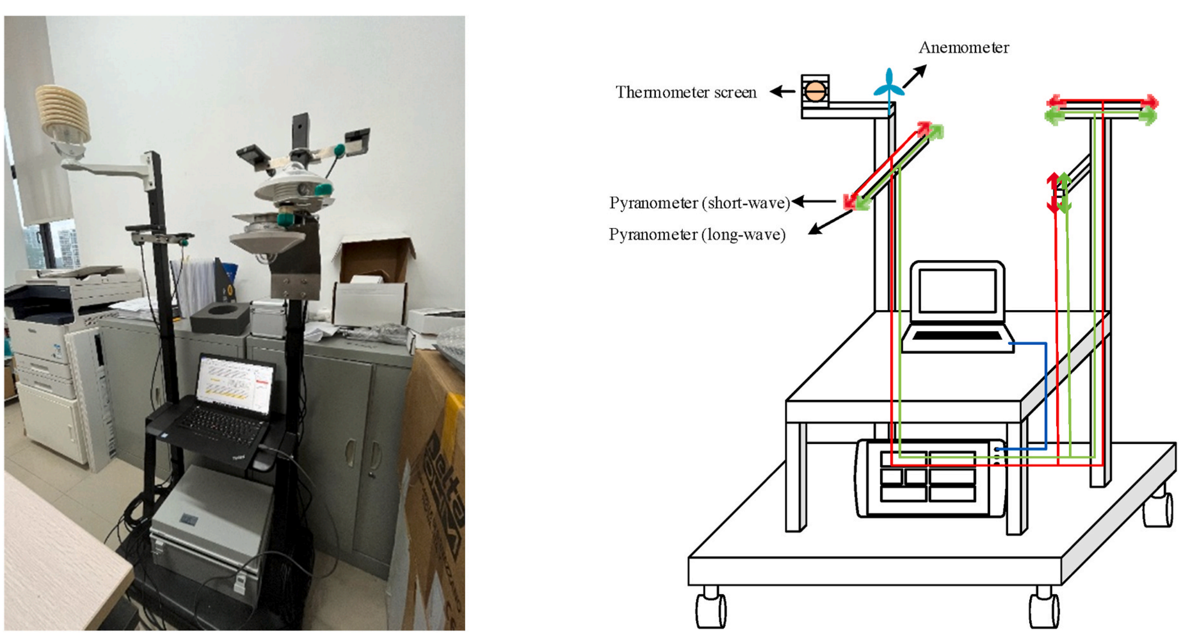

Fig. 2. Experiment instrument prototype and illustration.

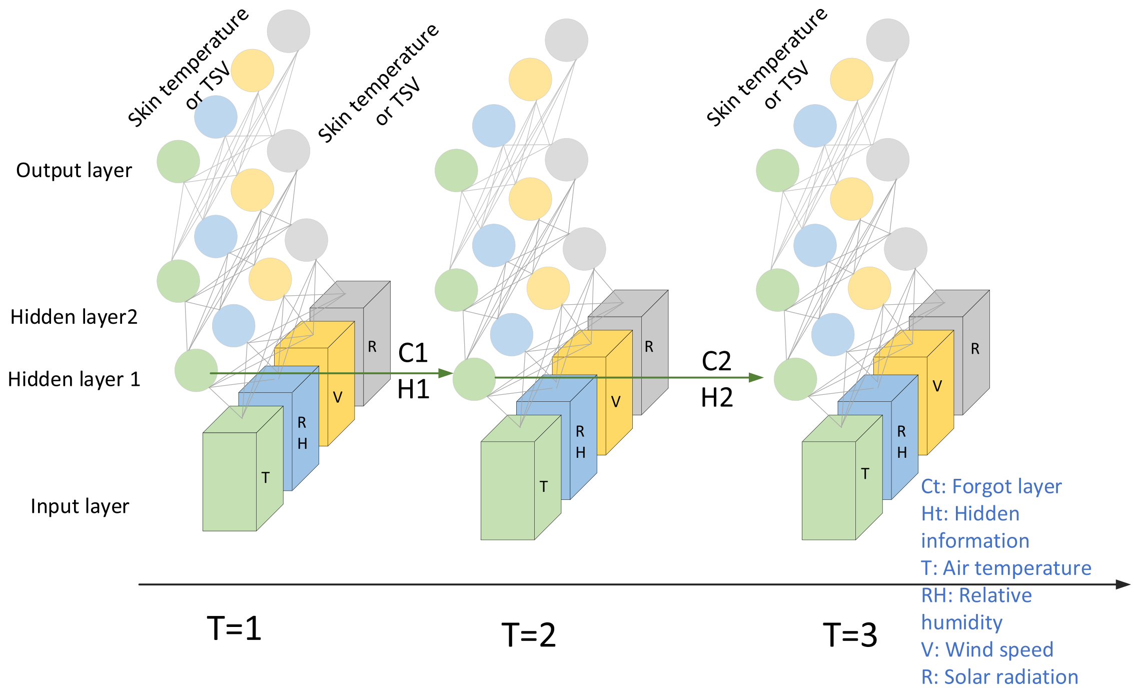

Fig. 3. LSTM diagram.

genetic algorithm was applied to tune hyper-parameters. The outcomes of this paper develop dynamic thermal comfort evaluations under solar radiation from the aspects of thermal physiology and psychology and can be utilized to assess outdoor thermal comfort with a comprehensive understanding of human factors.

2. Methods

2.1. Participants

A total of 15 participants were recruited in this study, including 7 males and 8 females, who were healthy and symmetrical. During the experiment, the participants wore uniform clothing to maintain clothing thermal insulation, about 0.6 clo (wearing a short-sleeved T-shirt and thin trousers). Respondents stood still at the site around the weather station. Demographic information is shown in Table 1.

2.2. Experimental process and test data

Intermittent solar radiation exposures were designed in the field experiment. A 5-min solar exposure followed by a 5-min shadow stay for three loops was set. The specific experimental process is shown in Fig. 1. The experimental site is selected on the square near a semi-open space, where respondents could switch between solar exposure and non-solar exposure quickly. In each experiment, two subjects participated, and eight groups of experiments were conducted. Before each experiment, subjects maintained a stationary position to ensure thermophysiological conditions stable.

Considering influences of solar radiation intensity and outdoor stay time on physiological parameters, the outdoor thermal environment parameters (solar radiation intensity, air temperature, relative humidity, wind speed) were tested every 10 s automatically. The experiment instruments are shown in Fig. 2. At the same time, the skin temperatures are continuously monitored. Skin temperatures were measured at five points, which are forehead, back, abdomen, back of the hand and calf. The test equipment and accuracy are listed in Table 2 and subjective questionnaires were filled every 1 min.

2.3. Subjective survey

During the experiment, participants were asked to fill in a questionnaire through mobile phone every minute. Overall local thermal sensation, solar exposure sensation, overall thermal comfort and overall thermal acceptance were interviewed. A seven-point scale for thermal sensation is adopted, which ranges from −3 to 3 (cold, cool, slightly cool, neutral, slightly warm, warm and hot) [48]. A four-point scale for solar exposure sensation is accepted, ranging from 0 to 3 (no solar exposure, slightly solar exposure, medium solar exposure, strong solar exposure) [49]. Thermal acceptance vote is scaled on a four-point scale (−2 unacceptable, −1 slightly unacceptable, 1 slightly acceptable, 2 acceptable) [50]. Thermal comfort vote ranges from 0 to 4 (comfort, slight discomfort, discomfort, quite discomfort, unbearable) [48]. Humidity and wind sensation vote were assessed on a four-point scale ranging from 0 to 3.

2.4. Outdoor thermal comfort index

To evaluate outdoor thermal comfort, PET and UTCI were compared with thermal sensations. PET is termed as the air temperature at which the core and skin temperature equal to those under the conditions being

Table 2
Instrument information.

	Type	Parameter	Precision	Range
Thermometer	HOBO U12-012	Air temperature	±0.35 °C	−20~70 °C
		RH	±2.5 %	5 % ~ 95 %
Anemometer	TJHY WFWZY1	Wind speed	5 % ± 0.05 m/s	0.05–30 m/s
Pyranometer	DELAOHM LPPYRA02S	Short-wave radiation	10μV/(W/m2)	0~2000 W/m2
Pyranometer	Apogee SL-510-SS	Long-wave radiation	0.12mV/(W/m2)	−200 to 200 W/m2
iButton	iButton DS1923	Surface temperature	±0.5 °C	−20~85 °C
Fitbit	Fitbit Inspire HR	Heartbeat		

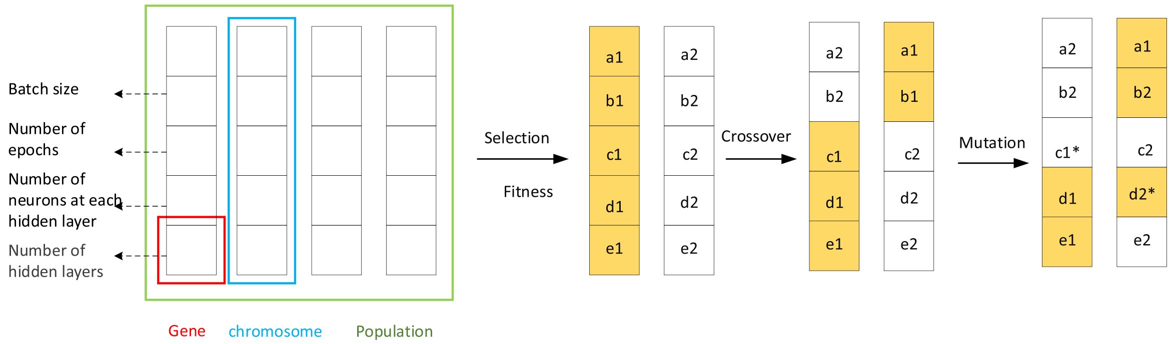

Fig. 4. Illustration of GA process.

Table 3
LSTM model configuration.

Network Parameter	Configuration
Number of hidden layers	1
Number of neurons at each hidden layer	251
Number of epochs	500
Learning rate	0.001
Activation function	ReLU
Weight initialization	Normal distribution
Loss function	MAE

assessed under heat balance state, which is founded on the Munich Energy-balance Model for Individuals (MEMI) [51]. PET has been verified in many field studies with good accuracy and is recommended by VDI (2008) [52]. UTCI was based on multidisciplinary knowledge of thermophysiology, medicine, biometeorological and environmental science. UTCI is represented by the reference air temperature (air temperature equal to MRT, wind speed = 0.5 m/s at 10 m, RH = 50 % up to a constant water vapor pressure of 20 hPa and metabolic rate = 135 W/m^2) that cause the identical thermal stress as the real environment. UTCI is developed from a multi-node dynamic thermophysiological model called UTCI-Fiala model [25].

The DTS model, based on Fiala's thermoregulatory models, allows for the prediction of thermal sensations in dynamic situations [42]. It has been validated under conditions of dynamic temperatures. The DTS model establishes a relationship between thermal sensation and several factors, including head core temperature, mean skin temperature, and the rate of change of mean skin temperature (dynamic signal). This relationship can be expressed through Equation (3).

Table 4
Metrics of model performance.

Index	Definition	Formular
RMSE	Average magnitude of the errors between predicted values and observed values.	$RMSE = \sqrt{\frac{\sum_{i=1}^{n}(y_i - \tilde{y}_i)^2}{n}}$
MAE	Average absolute differences between predicted values and observed values. It gives equal weight to all errors without considering their direction.	$MAE = \frac{\sum_{i=1}^{n}\lvert y_i - \tilde{y}_i\rvert}{n}$
R^2	Proportion of the variance in the dependent variable that is predictable from the independent variables.	$R^2 = 1 - \frac{\sum_{i=1}^{n}(y_i - \tilde{y}_i)^2}{\sum_{i=1}^{n}(y_i - \bar{y}_i)^2}$

Note: n is the number of data points, y_i is the actual value, $\tilde{y}_i$ is the predicted value, and $\bar{y}_i$ is the mean of the actual values.

$$DTS = 3 \times \tanh\left[a \bullet \Delta T_{sk,m} + F_2 + \left(0.11\frac{dT_{sk,m}^{(-)}}{dt} + 1.91_{e}^{-0.681t} \bullet \frac{dT_{sk,m}^{(+)}}{dt_{max}}\right) \bullet \frac{1}{1+F_2}\right] \tag{3}$$

Where a is regression coefficient, $\Delta T_{sk,m}$ is the error signal of mean skin temperature, °C, F_2 represents the influences of thermal strain caused by body core, $T_{sk,m}$ is the mean skin temperature, °C.

2.5. A GA-LSTM model

The long short-term memory network (LSTM) is novel recurrent neural network (RNN), integrated with an appropriate gradient-based learning algorithm (see Fig. 3). It features a unique "gate" structure consisting of an input gate, output gate, and forget gate. The purpose of these gates is to control the flow of information within the network. Whether data is updated or discarded is determined by the logic control of the gate unit, which mitigates the issues of a large weight in RNN. This

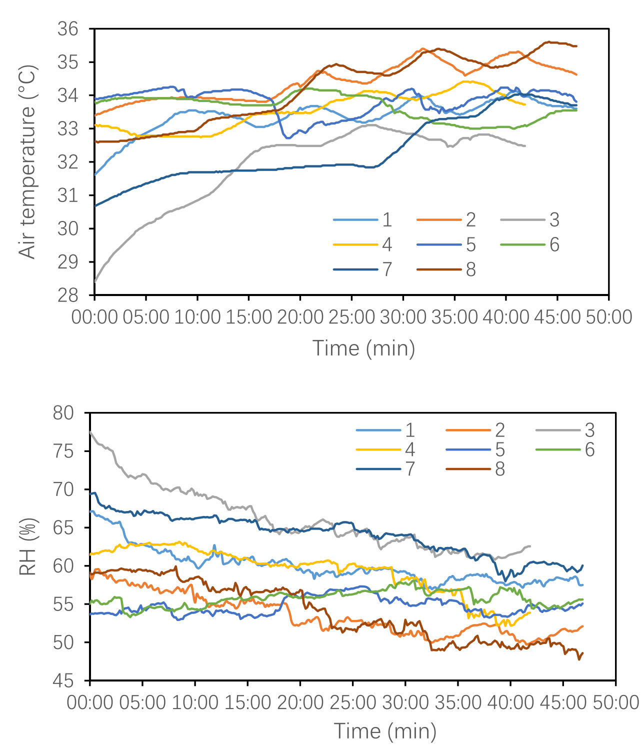

Fig. 5. Outdoor air temperature and relative humidity (a) air temperature, (b) relative humidity.

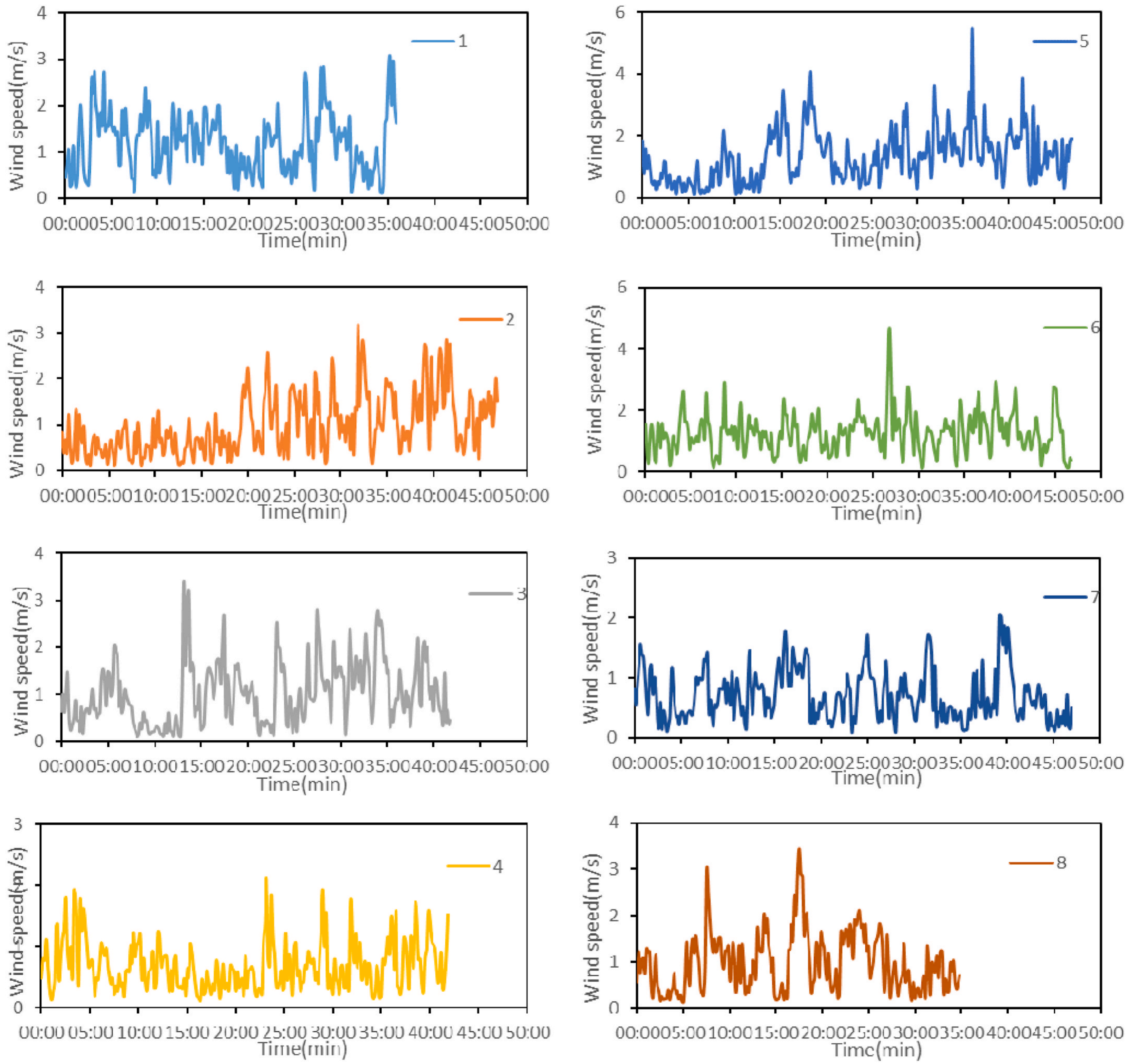

Fig. 6. Outdoor wind speed.

mechanism allows the LSTM network to better handle long-term dependencies and alleviate problems such as gradient disappearance and explosion that can occur in RNNs.

The LSTM network's gate structure enables it to converge more effectively and quickly, leading to improved prediction accuracy. By selectively retaining or forgetting information, the network can maintain and update relevant information over longer sequences, making it particularly suitable for tasks involving time series or sequential data.

Data transformation is important for neural network training, which can accelerate the training speed with a good performance. One good data transform suggests the transformation of data to be within the same range as output of the activation function that is used in the model training. The Rectified linear unit (ReLU) is the most widely used activation function in the training of the neural network. It is provided by default from PyCharm environment, and its derivative values are between 0 and 1. A good scaling for the data is to transform it to fall within the same range. The MinMaxScaler function provided by sklearn preprocessing library is used for this.

The data is then transformed into a supervised data (input and output patterns). The previous observations of the previous time step are used as an input to the network at the current time step.

Before training LSTM model, some hyper-parameters should be determined by tests, such as number of hidden layers, and number of neurons at each hidden layer. Genetic Algorithm (GA) is an adaptive probabilistic global search algorithm, which is based on the principles of natural selection and genetics, and draws on the natural selection mechanism of biological evolutionary superiority and inferiority, and the genetic mechanism of recombination and mutation, as shown in Fig. 4. In GA, a set of initial populations (initial solutions) is first randomly generated, and this population consists of a certain number of individuals that have been genetically encoded. Each individual is a chromosome (the main carrier of the genetic information) bearing a

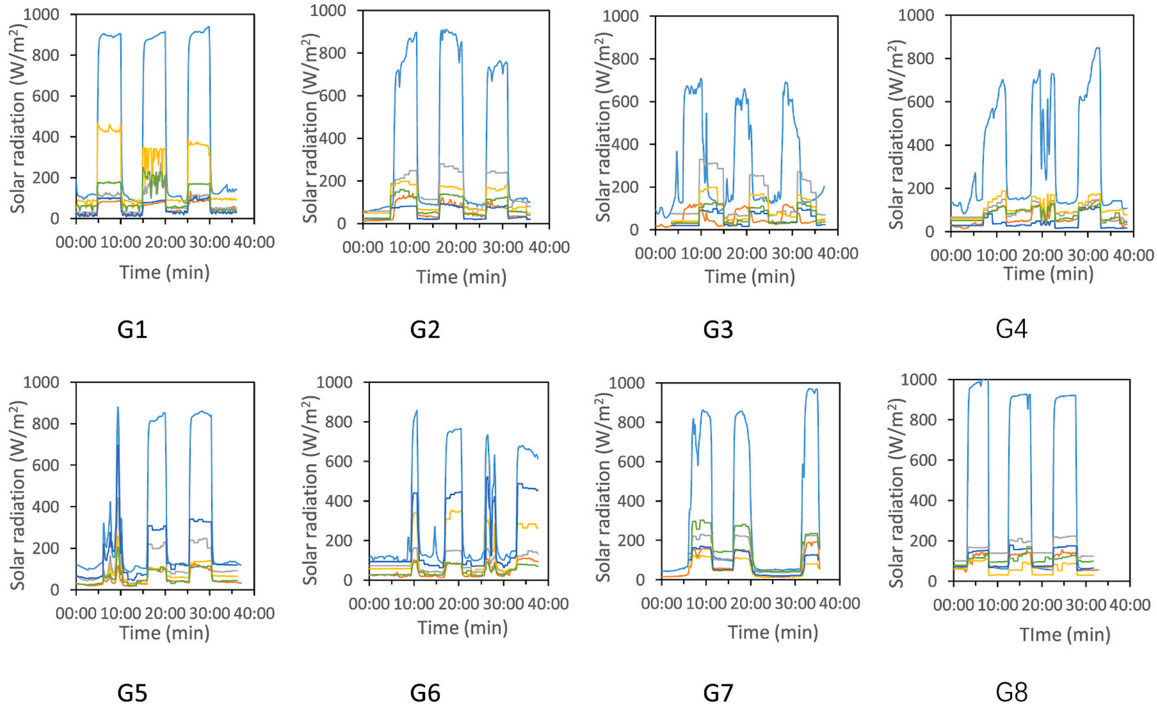

Fig. 7. Variations of global solar radiation.

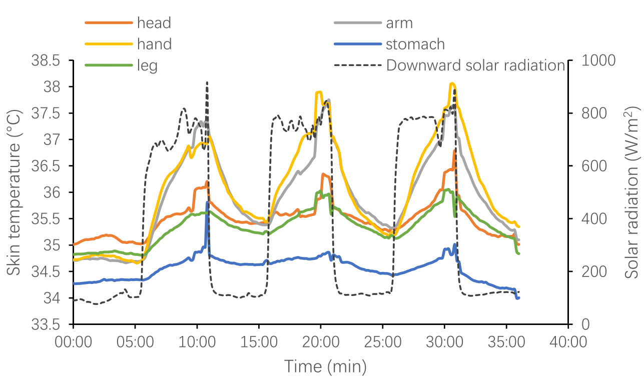

Fig. 8. Variations of skin temperature and downward solar radiation.

characterized entity, and the appearance of an individual is determined by its internal manifestation, i.e., genotype. After the initial population is generated, more optimal approximate solutions will evolve generation by generation according to the principle of superiority and inferiority. Eventually, the optimal individual of the final population can be used as the approximate optimal solution of the problem after decoding. The model parameters are given in Table 3.

Five-fold cross validation was applied to test the performance and stability of each parameter setting where the value of one parameter is changed within a specific range and the others are kept fixed. The fold that generates the best accuracy will use its configuration as optimal choice for the investigated parameter. The k-fold cross validation is a re-sampling method which divides the original dataset into k groups, and each sub-dataset will be used as a validation set. The model is trained and tested in different subsets of data in order to evaluate the model performance on the validation set.

In this study, we applied the GA-LSTM model to predict average skin temperature and overall thermal sensation. In this model, the inputs are environmental condition, including air temperature, relative humidity, wind speed and solar radiation. Through the deep learning model, time series data of average skin temperature and overall thermal sensation can be predicted.

Root mean squared error (RMSE), mean absolute error (MAE), R square (R2) is adopted to indicate the accuracy of model predictions. Table 4 summarizes the definitions and formulaes of the three model performance indicators.

RMSE can be used when large errors exist in predictions because RMSE penalizes large errors by squaring process, however, MAE is not reasonable when outliers have a critical influence on the performance evaluation. In addition, when errors are normally distributed, RMSE is more appropriate than MAE. R^2 often assesses the fitness of a regression model. However, it may not be suitable for models where prediction accuracy is the primary concern. In practice, multiple metrics instead of only one metric can provide a more comprehensive view of the model performance. For instance, with an integrated consideration of RMSE and R^2, model prediction accuracy and explanatory power can be analyzed. In general, the selection of metrics should comply with the objectives of model performance.

3. Experimental results

3.1. Outdoor objective environmental parameters

3.1.1. Air temperature, relative humidity, and wind speed

The air temperature and relative humidity during the five experimental tests are shown in Fig. 5. In groups 1 and 2, the air temperature ranged from 28.5 to 30.0 °C, while in groups 3 to 5 the air temperature range varied from 32.3 to 34.1 °C. The maximum temperature change in the five groups was 1.1 °C, and the standard deviations were 0.09, 0.43, 0.33, 0.28, and 0.34 °C, respectively. The variation range of relative humidity was between 52 % and 61 %. Although there were some fluctuations, the overall range of variation was relatively small.

3.1.2. Wind speed

Fig. 6 illustrates wind speed of the eight experiment groups. The wind speed mainly varies between 0.34 and 1.81 m/s, without a discernible pattern over time. The distributions of wind speed in groups

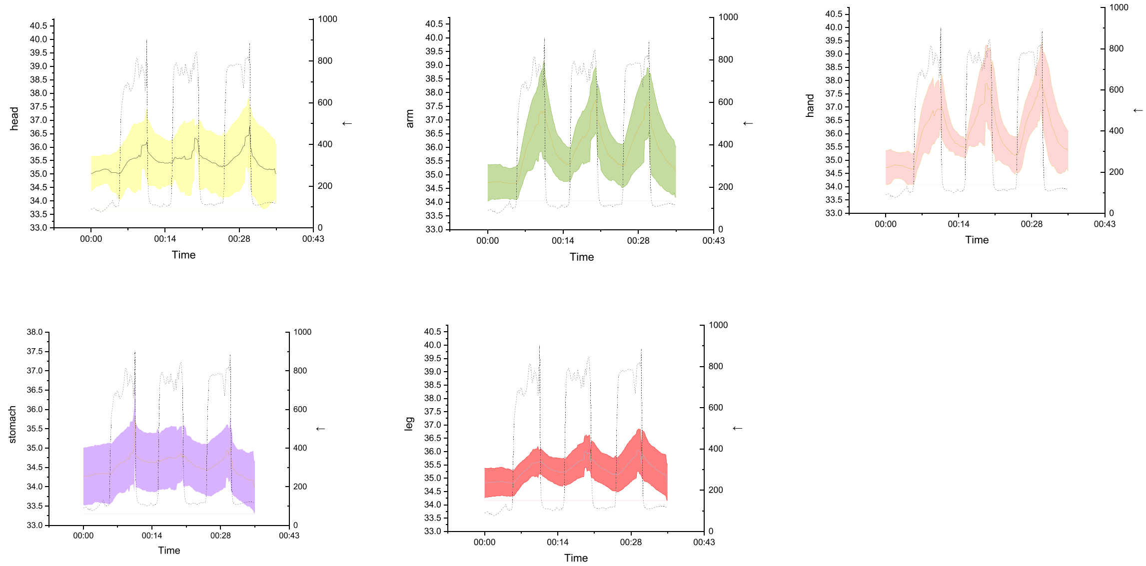

Fig. 9. Local skin temperature variations.

Table 5
Mean value of long-wave radiation (Unit: W/m^2).

Group No.	Downward	Upward	Leftward	Rightward	Forward	Backward
1	427.66	517.48	496.28	502.58	490.14	496.36
2	421.46	517.50	496.10	502.52	489.95	496.16
3	422.47	518.51	496.05	503.29	489.50	496.11
4	419.50	521.01	496.00	502.74	489.45	496.06
5	419.51	520.99	495.96	502.72	489.79	495.98
6	419.50	521.01	496.00	501.74	489.45	496.06
7	419.46	520.99	495.93	502.70	489.71	495.98
8	419.58	520.97	495.83	502.56	489.60	495.92

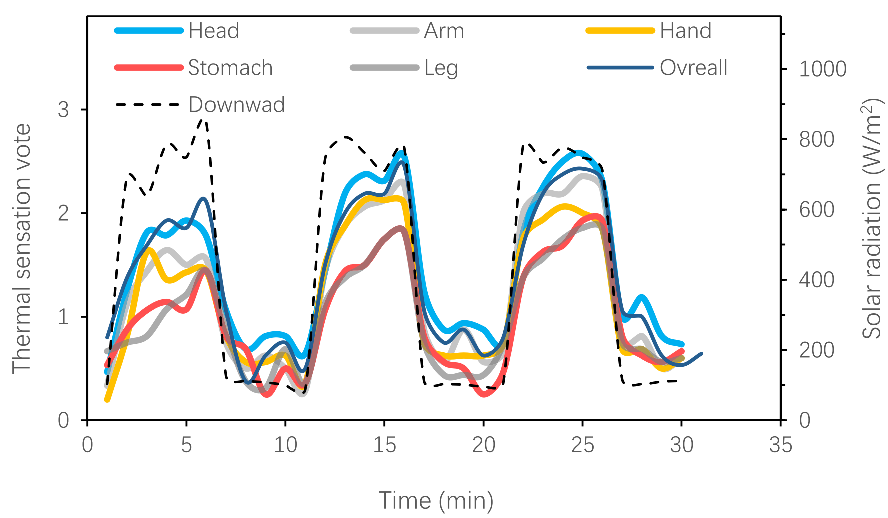

Fig. 10. Thermal sensation and solar radiation sensation.

1, 2, 7 and 8 are similar, and groups 4, 5, and groups 3, 6 have a similar distribution, respectively.

3.1.3. Global solar radiation intensity and long-wave radiation

Solar radiation intensity is an important factor affecting outdoor thermal comfort. The variation values of global solar radiation in the eight groups of experiments are shown in Fig. 7, which were measured in an interval of 10 s. The global solar radiation intensity of groups 1, 2, 4, 5, 6, 7, 8 is relatively high around 800–900 W/m^2, and the global solar radiation intensity in groups 3 and 4 is about 600, 700 W/m^2,

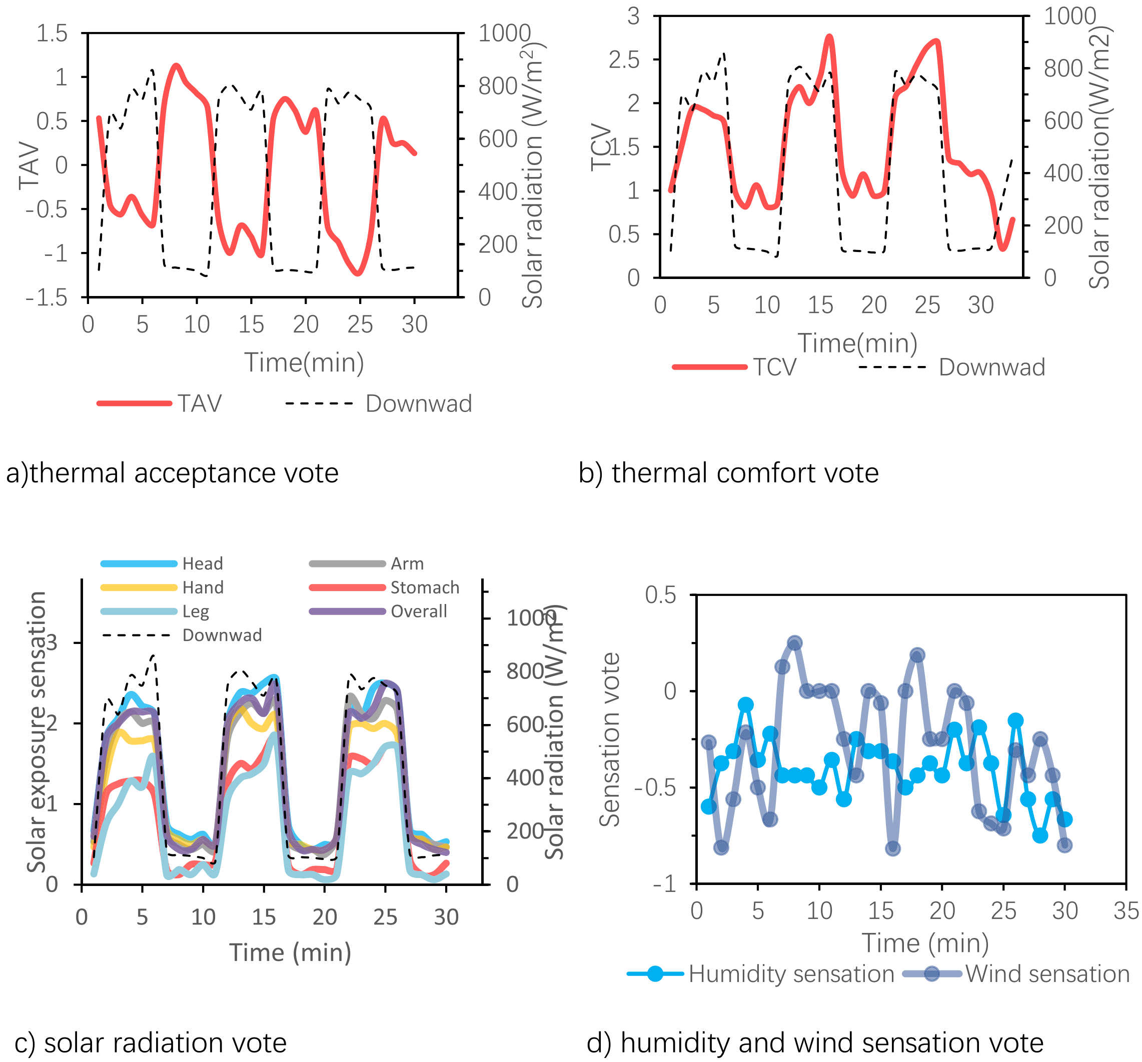

Fig. 11. Thermal responses variations with solar radiation (a) thermal acceptance vote, (b) thermal comfort vote, (c) solar exposure sensation vote, (d) humidity and wind sensation vote.

respectively. Due to the shading of clouds, the global solar radiation intensity is relatively low in the solar exposure stage. During the shadow stage, the global solar radiation mainly varied between 100 and 150 W/m^2.

Long-wave radiation is relative stable compared with solar radiation, and there is no significant difference under direct solar radiation exposure and non-direct solar radiation exposure. Table 5 summarizes the mean value of long-wave radiation. Upward long-wave radiation is obviously larger than downward long-wave radiation. The horizontal long-wave radiations are similar.

3.2. Changes of human skin temperature

During the experiment, the skin temperatures of the subject's head, abdomen, arms, hand and calf were measured to analyze the skin temperature variation under dynamic solar radiation exposure. After comparing the skin temperature at different body parts, it is evident that the skin temperature at arm and hand changes significantly with temperature fluctuations of 3.1 and 3.4 °C. In contrast, the changes at other parts (head, abdomen, leg) are relatively small, among which the skin temperature in the calf has the smallest change of 1.2 °C.

Due to the body thermal regulations (mainly due to evaporative heat dissipation caused by sweating, as well as blood flow regulation and metabolic regulation), the temperature of the human skin may decrease during the solar radiation exposure phase. When sweating is not present, there is a time delay in the skin temperature of unobstructed body parts (such as arms) after the sun exposure phase stops, but when there is thermophysiological regulation such as sweating, the human skin temperature is appropriately reduced.

3.3. Subjective psychological evaluation of the human body

The thermal sensation variations of the whole body and different segments of the human body under intermittent solar radiation exposure are shown in Fig. 10. Thermal sensations of head, arm, and hand are higher than thermal sensations of leg and stomach. Overall thermal sensations are closer to thermal sensations of the head, which is the most sensitive. The thermal sensations of various parts of the human body have the same trend as that of the skin temperature. This means that as the body skin temperature increases, the thermal sensation votes also become higher.

As Fig. 11a) and b) shows, high solar intensity will cause thermal discomfort and low thermal acceptance. Thermal comfort and thermal acceptance changes in accordance with solar radiation in the scale of time. When solar exposure became intense, people would immediately feel uncomfortable and slightly unacceptable. For thermal acceptability,

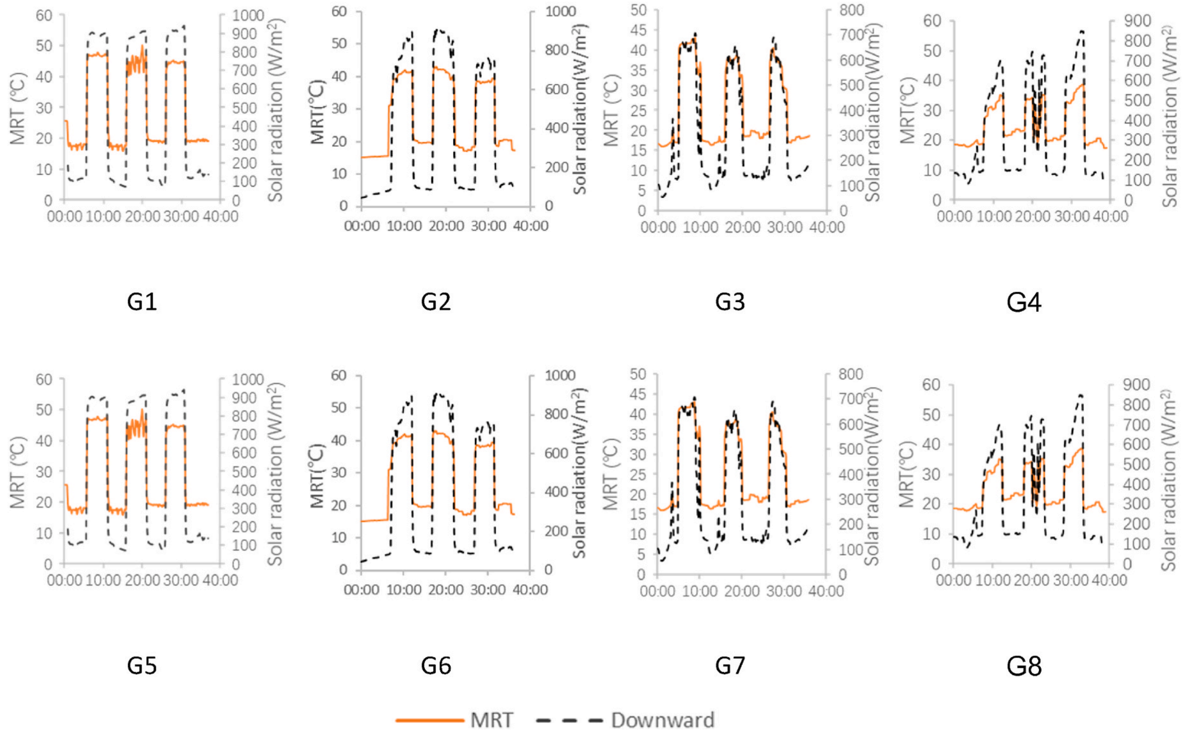

Fig. 12. MRT and downward solar radiation.

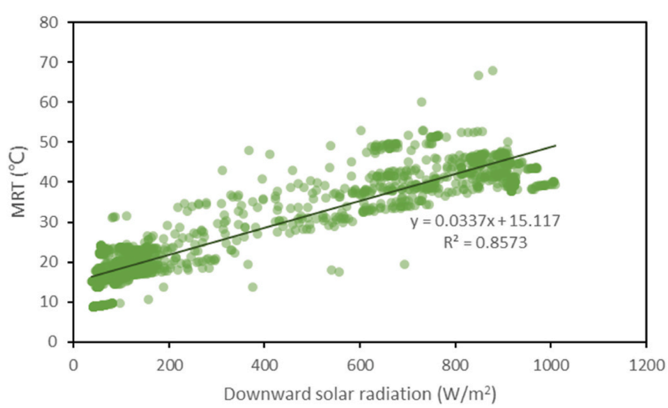

Fig. 13. The regression relationship between MRT and solar radiation.

participants would have an over high unacceptability once they came into solar exposure. Later they may have adaptations to the solar exposure and acceptance increases a little. But solar exposure at last would cause high unacceptance. Similarly, when people come into the shadow zone, they will have comfort and acceptability fluctuations.

Solar exposure sensation votes (SESV) in overall, head, arm, and hand show that a great consistency with solar radiation, while sensations at stomach and leg are less sensitive to solar radiation changes. Compared with thermal sensations, people have a less reaction time to solar exposure change, especially at the naked segments. Similar to thermal sensations, overall SESV was greatly influenced by the strongest local SESV. Humidity sensation and wind sensation varies with little relationship to solar exposure change as Fig. 11d) shows.

3.4. Mean radiant temperature and downward solar radiation

Mean radiant temperature (MRT) was calculated according to "Six-direction method", as Equations (4)–(6) show. This method applies short-wave radiation and long-wave solar radiations of six directions.

$$Tmrt = \sqrt[4]{\frac{K_{abs} + L_{abs}}{\alpha_l \bullet \sigma}} - 273.15 \tag{4}$$

$$K_{abs} = \alpha_k \bullet \sum_{i=1}^{6} W_i \bullet K_i \tag{5}$$

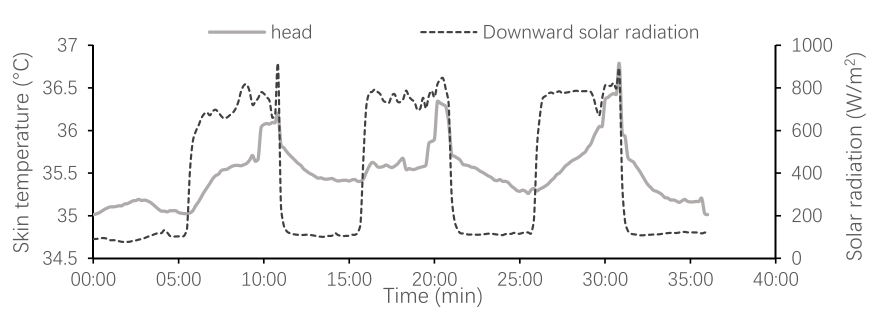

Fig. 14. Variation of skin temperature and solar radiation.

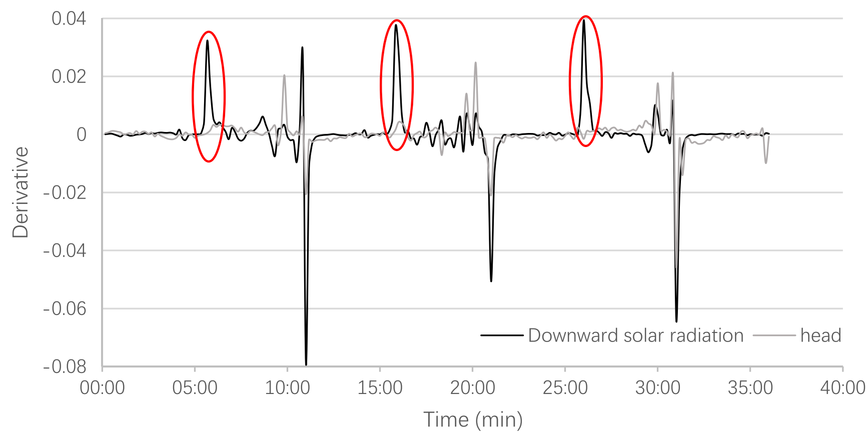

Fig. 15. Variation of first derivative of skin temperature and solar radiation.

$$L_{abs} = \alpha_l \bullet \sum_{i=1}^{6} W_i \bullet L_i \quad (6)$$

where,

T_{mrt} Mean radiant temperature , °C.

K_{abs} Total short-wave radiation , W/m^2

L_{abs} Total long-wave solar radiation , W/m^2

σ Boltzmann constant , 5.67×10^{-8} $W/(m^2K^4)$.

α_l Absorption coefficient of long-wave radiation, equal to 0.97

α_k Absorption coefficient of short-wave radiation, equal to 0.70

W_i Angle coefficients of six directions. 0.06 for the two vertical directions and 0.22 for the four horizontal directions

K_i, L_i Short-wave radiations and long-wave radiations of six directions

As Fig. 12 shows, MRT varies significantly under solar radiation and non-direct solar radiation conditions. It seems there is a strong relationship between MRT and downward solar radiation, thus, we developed a linear regression model between them as Fig. 13 shows. In some cases of instrument lack, MRT can be estimated by down-ward solar radiation.

4. Analysis of the impact of dynamic solar radiation exposure on physiology and psychology

4.1. Influence of dynamic solar radiation on thermophysiology

As Fig. 8 shows, the skin temperatures change with solar radiation, especially at the exposed segments. Unlike a sudden change of solar radiation, the skin temperatures rise or fall gradually. Due to differences of the physiological properties of skin tissue across the body, the fluctuations of different body segments vary. When the heat exchange between the human body and the surrounding environment cannot reach a balance, the body will perform thermal regulations. When exposed to sunlight, the body's skin capillaries regulate blood flow by constricting or dilating, thereby managing heat exchange. Additionally, sweating plays a crucial role in heat regulation. During self-heat regulation, the skin temperature decreases. For example, after repeated sun exposure, the skin temperature of the head, backs of hands, and calves decreased earlier, possibly due to the effects of sweating.

Fig. 14 emphasizes the changes of skin temperature of head and solar radiation. There exists a time lag between solar radiation and skin temperature when people come into solar exposure. However, when people leave solar exposure, the skin temperature drops quickly as solar radiation. To further analyze the time lag between solar radiation and skin temperature, the first derivatives of the two parameters were calculated as shown in Fig. 15. A time lag between solar radiation and skin temperature is obvious from the first derivatives changes, which is about 20 s.

4.2. Influence of dynamic solar radiation on thermal psychology

According to Fig. 10, thermal sensations have a good accordance with solar radiation, particularly for head, arm, and hand. Therefore, exposed segments demonstrate a strong response to solar radiation. The rate of change in TSV differs during the increasing and decreasing solar radiation period. The thermal sensation increases slowly when solar radiation increases, while it dumps sharply from solar radiation to non-solar radiation. After approximately 1–2 min of exposure to solar radiation, thermal sensations will reach a peak and become stable.

From solar exposure to non-solar exposure, both the skin temperature and TSV drops rapidly. When people enter solar exposure, their skin temperature will rise at a slower rate compared to TSV. Therefore, relying solely on skin temperature is not enough to predict thermal sensation, unless considering the derivatives of skin temperatures.

5. Predicted skin temperature and thermal sensation model based on LSTM model

5.1. Model establishment and validation

Here we adopted LSTM model to establish a prediction model on average skin temperatures (numerical average of five body parts' skin temperature), applying thermal environmental parameters (air temperature, relative humidity, wind speed and global solar radiation) as model inputs to predict skin temperature with a time step of 10s, and the five-fold cross validation results are given in Fig. 16. A total of 220 data samples were used to train the model. The predicted skin temperatures are in accordance with experiment data with RMSE ranging from 0.038 to 0.050. The LSTM-based model has a good performance in predicting skin temperatures.

Thermal sensations under dynamic solar exposure are predicted though LSTM model. Although thermal sensation is scaled from −3 to 3, the magnitude of thermal sensation vote is meaningful. Besides, a lot of linear regression model have been developed to reveal the thermal sensations and thermal environments. Actually, in LSTM model, thermal sensation vote is considered as a continuous variable.

The four thermal environmental variables are model inputs here as well with a time step of 1 min in accordance with thermal sensation vote. A total of 480 data samples were used to develop the model. However, here only 2/3 of the original data were trained with LSTM model. The left data was used to validate the model accuracy. The model performance is shown in Fig. 17. Although RMSEs ranging from 0.699 to 1.027 shows a significant error, the predicted thermal sensation has a similar trend with experiment data. Lack of database or inappropriate inputs

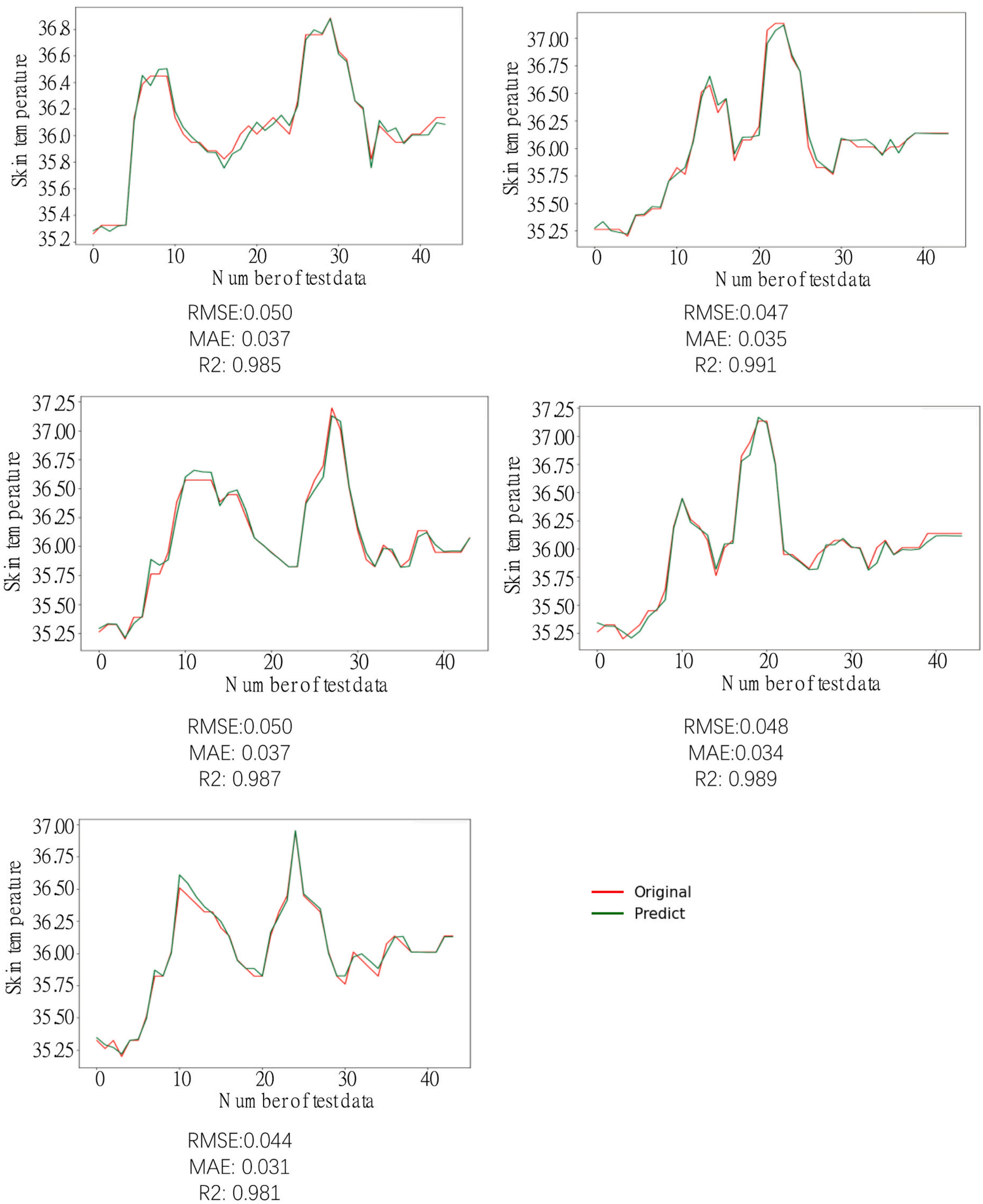

Fig. 16. Performance of skin temperature prediction model.

may lead to the result. Besides, unlike the strong theoretical relationship between skin temperature and thermal environment (Heat transfer between human body and thermal environment follows the Fourier laws), thermal sensation may be also influenced by human thermal adaptation. This may aggravate the error between the predicted and the original data.

To test the model accuracy, five original sub-datasets are compared with predicted thermal sensations shown in Fig. 18. RMSEs between predicted and validated data are 0.084, 0.140, 0.175, 0.296, and 0.263, which has quite good performance. This may be caused by model overfitting or data distribution discrepancy between test and validated data. To solve the above problem, model parameter adjustments and database expansion may improve the model performance.

5.2. Comparison between thermophysiological model and LSTM model

Fiala developed a dynamic thermal sensation model (DTS), which is derived from a relationship between time series of thermal sensation votes from experiments with dynamic physiological parameters predicted by Fiala multi-node thermoregulation model [42]. The regression was performed taking into account the nonlinear trend of measured sensation votes when thermal sensation approaches asymptotically the

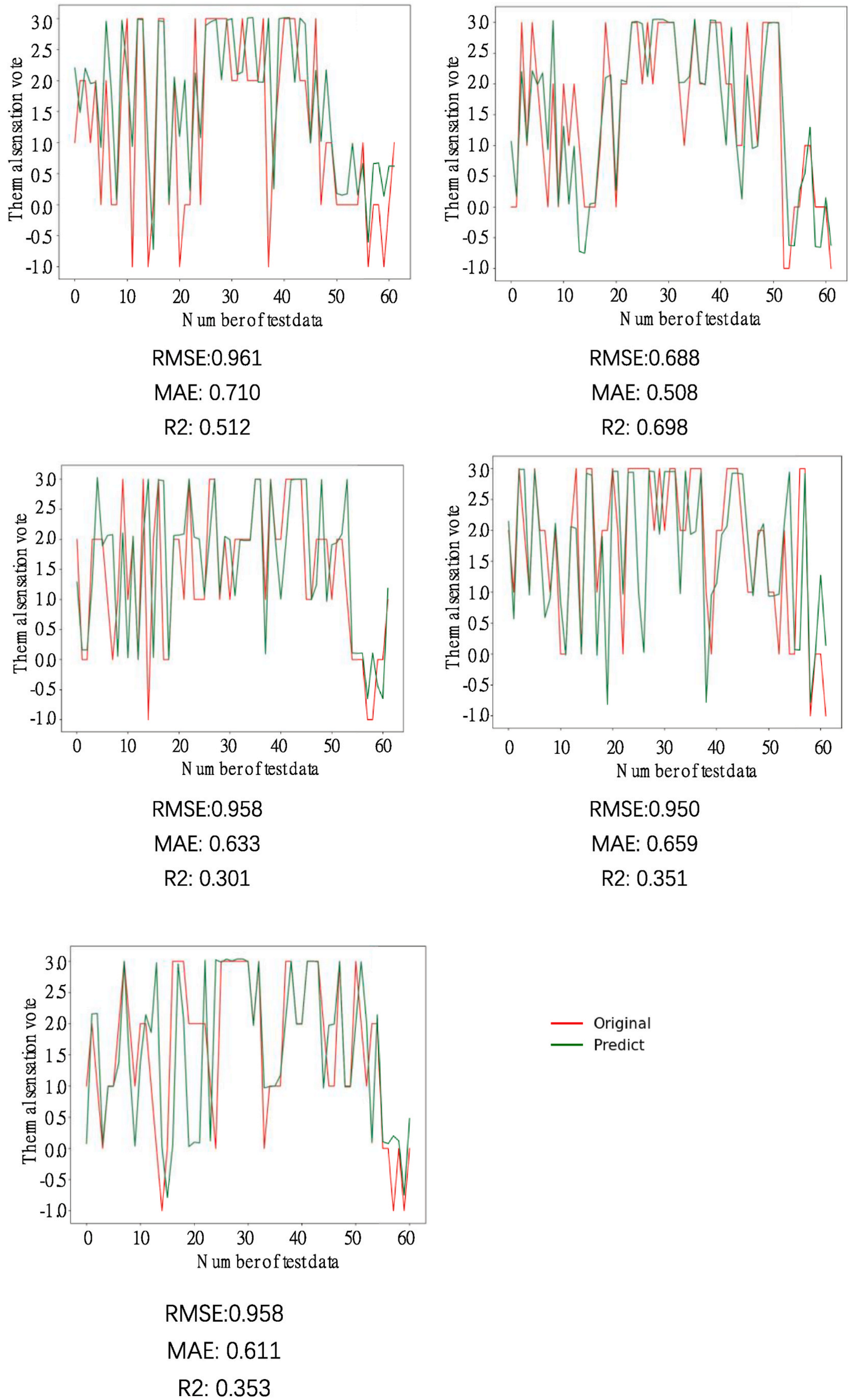

Fig. 17. Performance of thermal sensation prediction model.

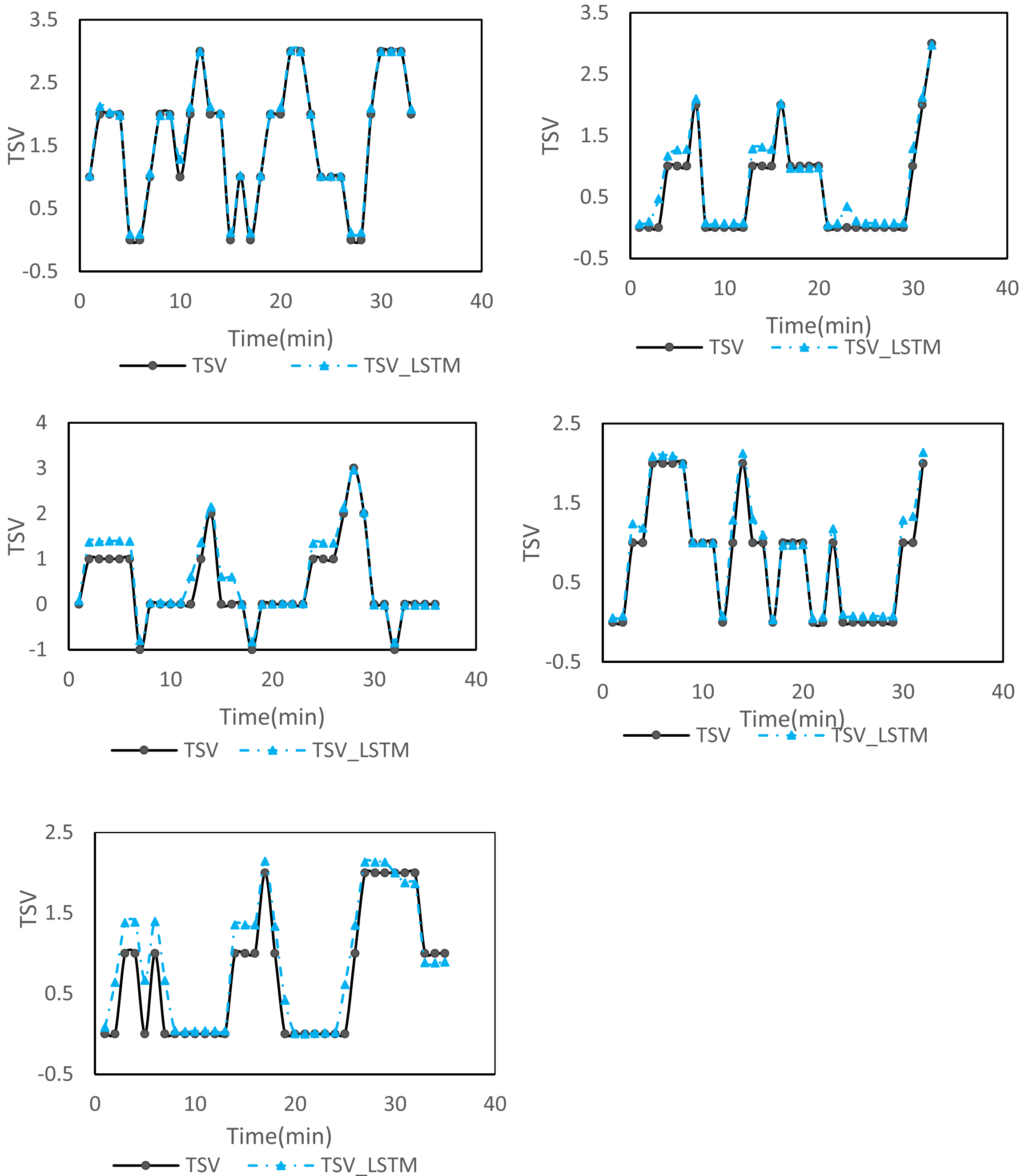

Fig. 18. Comparison between predicted and original thermal sensations.

lower and upper limit of the ASHRAE 7-point scale.

Based on measured skin temperatures, DTS can be generated. The comparisons between DTS and LSTM-predicted thermal sensation are shown in Fig. 19.

As Fig. 19 shows, LSTM model has a better performance in predicting dynamic thermal sensation compared with DTS model by comparing the average difference. DTS model has an obvious time lag with real thermal sensations. This is maybe caused by non-Fourier heat transfer in skin tissues, which would lead to a time lag of skin temperature. As Equation (1) shows, DTS is determined by skin temperatures. Thus, DTS would have a time lag with thermal sensations with real sensations.

6. Discussion

6.1. Applicability of existing thermal comfort indexes

Although PET and UTCI are two popular outdoor thermal comfort evaluation indexes, they are unknown for applications in dynamic solar radiation conditions. Both PET and UTCI vary significantly between solar condition and non-solar condition, which is similar to variations of MRT.

To check the applicability of PET and UTCI in dynamic conditions, weighted linear regression analysis between PET or UTCI and mean thermal sensations (MTS) is shown in Fig. 20. The linear regression models between PET or UTCI and MTS shows a positive relationship.

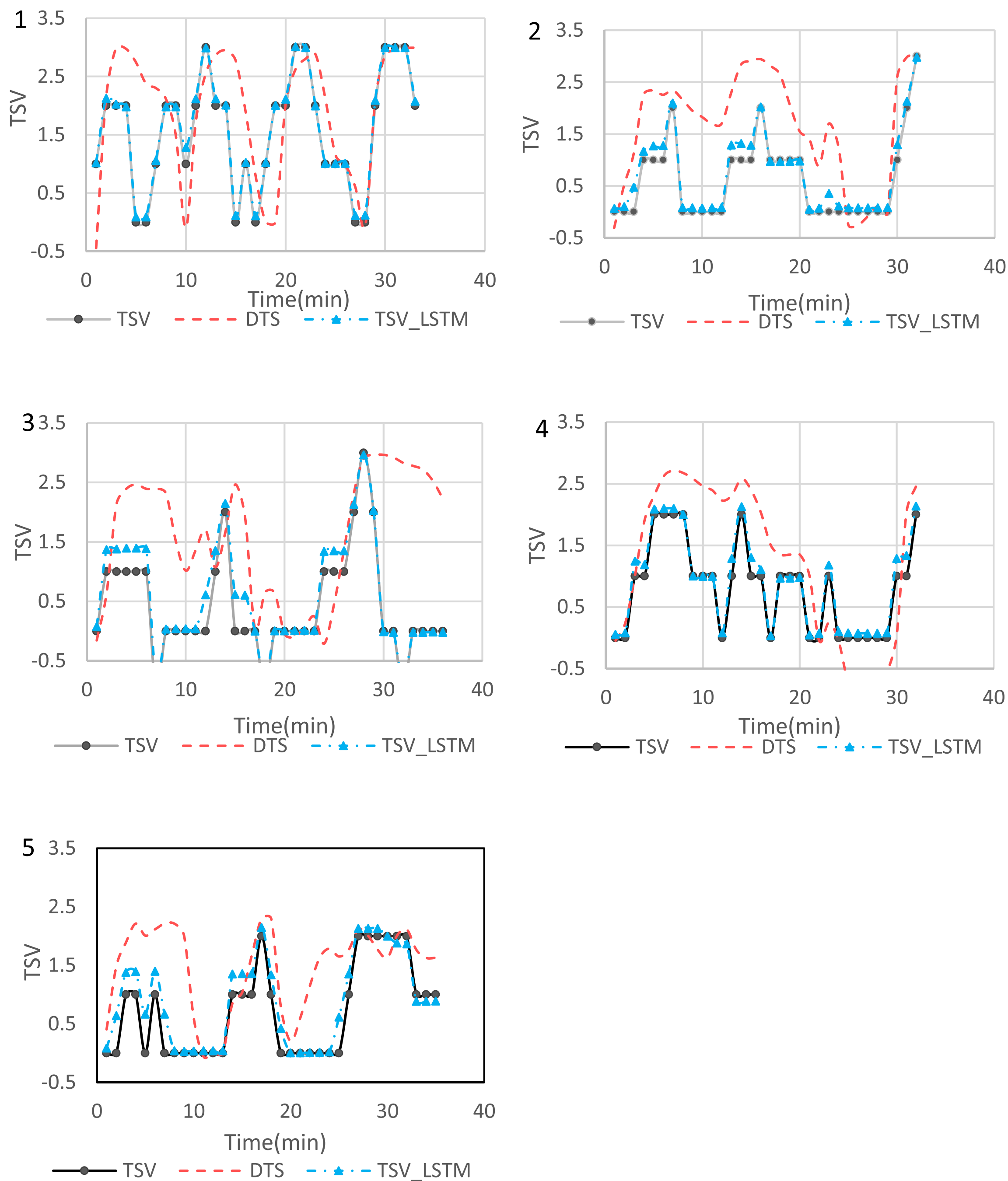

Fig. 19. Comparison between DTS and LSTM model.

UTCI has a better correlation with thermal sensations with R^2 of 0.725. Therefore, UTCI has a better correlation with thermal sensations than PET.

6.2. Correlation and sensitivity of thermal sensations and skin temperature to solar radiation

Through a paired *t*-test, the differences between overall and local thermal sensations were analyzed, as shown in Table 6. The overall thermal sensations have a significant difference with local thermal sensations except head under $p < 0.01$, which means that overall thermal sensations may be greatly influenced by thermal sensation at the head.

Overall thermal sensations obey the 'Complaint model', which indicates overall thermal comfort was determined by the most uncomfortable body segment. As Fig. 9 shows, thermal sensation vote at head is the highest, which would significantly influence overall thermal sensation.

Furthermore, it is worth noting that the thermal sensations at the stomach and leg segments are relatively close to each other, possibly indicating similar levels of thermal comfort for these body parts.

To figure out the sensitivity of overall and local thermal sensation to solar radiation intensity, the Pearson's coefficients are given in Table 7. The overall thermal sensation has the strongest correlation with solar radiation. The head, arm and hand thermal sensations have a stronger correlation with solar radiation than thermal sensations at stomach and

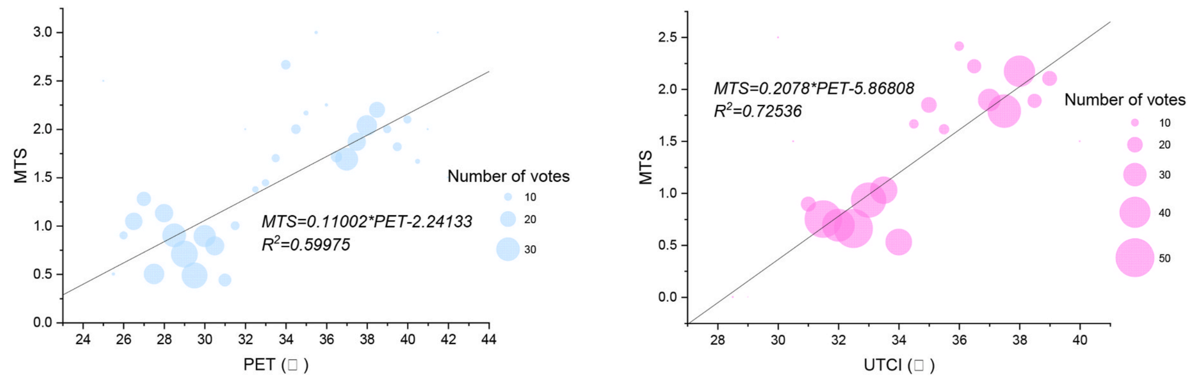

Fig. 20. PET and UTCI with thermal sensation.

Table 6
Variance analysis of overall and local thermal sensations.

	Overall	Head	Arm	Hand	Stomach	Leg
Overall	–	–	–	–	–	–
Head	0.023	–	–	–	–	–
Arm	0.000	0.000	–	–	–	–
Hand	0.000	0.000	0.011	–	–	–
Stomach	0.000	0.000	0.000	0.001	–	–
Leg	0.000	0.000	0.000	0.001	0.788	–

leg, which may be caused by clothing cover. Head, arm, and hand are directly exposed to the sun, and stomach and leg are covered with clothes. Therefore, thermal sensations at the stomach and leg may have a low amplitude and a time lag with solar radiation variations.

Based on variance analysis, local skin temperatures are found to be significantly different. Pearson's coefficients between local skin temperatures and solar radiation are given in Table 8. Local skin temperatures have a strong inter-relationship. Solar radiation has stronger correlations with head, arm, and hand, compared with stomach and leg, which is similar to the relationship between solar radiation and local thermal sensations.

In general, both thermal sensations and skin temperatures at exposed body segments show a stronger correlation to solar radiation.

7. Conclusion

In this paper, our focus was on dynamic thermal comfort during step-change solar radiation exposures. We analyzed the variations in thermal psychological and physiological responses to explore the time discrepancy between human responses and thermal environment parameters. The main conclusions in this study are as follows.

(1) Skin temperatures change with solar radiation, especially at the exposed segments. There exists a time lag between solar radiation and skin temperature when people come into solar exposure. However, when people leave solar exposure, the skin temperature drops quickly as solar radiation.
(2) The thermal sensation gradually increases as solar radiation rises, but when transitioning from solar radiation to non-solar radiation, it drops sharply. After approximately 1–2 min of exposure to solar radiation, thermal sensations will reach a peak and stabilize.
(3) Both thermal sensations and skin temperatures at exposed body segments show a stronger correlation to solar radiation.
(4) From solar exposure to non-solar exposure, both the skin temperature and TSV drops rapidly. When people enter solar exposure, their skin temperature will rise at a slower rate compared to TSV. Therefore, relying solely on skin temperature is not enough to predict thermal sensation under dynamic solar exposure, unless considering the derivatives of skin temperatures.
(5) Based on a GA-LSTM model, a skin temperature prediction model and a thermal sensation prediction model were established. The predicted skin temperature is in accordance with experiment data with RMSE below 0.05 while the predicted thermal sensations have a significant difference with original data. Compared with thermophysiological models (DTS), LSTM model has a better prediction accuracy in thermal sensations.
(6) Under dynamic solar radiation, thermal sensation vote at head is the highest, which would significantly influence overall thermal sensation. Thermal sensations at the stomach and leg may have a low amplitude and a time lag with solar radiation variations.

Table 8
Correlation between local skin temperatures and solar radiation.

	Head	Arm	Hand	Stomach	Leg	Solar radiation
Head	1.000					
Arm	0.933	1.000				
Hand	0.890	0.972	1.000			
Stomach	0.837	0.777	0.706	1.000		
Leg	0.863	0.947	0.957	0.700	1.000	
Solar radiation	0.611	0.590	0.601	0.573	0.466	1.000

Table 7
Correlation analysis of thermal sensation and solar radiation intensity.

	Overall	Head	Arm	Hand	Stomach	Leg	Solar radiation
Overall	1.000						
Head	0.975	1.000					
Arm	0.970	0.981	1.000				
Hand	0.950	0.975	0.978	1.000			
Stomach	0.953	0.950	0.960	0.938	1.000		
Leg	0.955	0.940	0.950	0.932	0.973	1.000	
Solar radiation	0.923	0.890	0.912	0.902	0.866	0.850	1.000

CRediT authorship contribution statement

Yuchen Ji: Writing – original draft, Visualization, Validation, Methodology, Investigation, Formal analysis, Data curation, Conceptualization. **Jusheng Song:** Supervision, Project administration. **Pengyuan Shen:** Writing – review & editing, Supervision, Resources, Methodology, Funding acquisition, Conceptualization.

Declaration of competing interest

The authors declare that they have no known competing financial interests or personal relationships that could have appeared to influence the work reported in this paper.

Data availability

Data will be made available on request.

Acknowledgement

This work is partly supported by the National Natural Science Foundation of China (NSFC) (Grant No. 52008132).

References

[1] M. Kappelle, WMO Statement on the State of the Global Climate, 2019, p. 2020.
[2] P. Shen, Impacts of climate change on U.S. building energy use by using downscaled hourly future weather data, Energy Build. 134 (2017) 61–70.
[3] P. Shen, M. Wang, J. Liu, Y. Ji, Hourly air temperature projection in future urban area by coupling climate change and urban heat island effect, Energy Build. 279 (2023), 112676.
[4] P. Shen, J. Liu, M. Wang, Fast generation of microclimate weather data for building simulation under heat island using map capturing and clustering technique, Sustain. Cities Soc. 71 (2021), 102954.
[5] M. Santamouris, D. Kolokotsa, On the impact of urban overheating and extreme climatic conditions on housing, energy, comfort and environmental quality of vulnerable population in Europe, Energy Build. 98 (2015) 125–133.
[6] D. Founda, M. Santamouris, Synergies between urban heat island and heat waves in Athens (Greece), during an extremely hot summer (2012), Sci. Rep. 7 (1) (2017), 10973.
[7] M. Zinzi, S. Agnoli, C. Burattini, B. Mattoni, On the thermal response of buildings under the synergic effect of heat waves and urban heat island, Sol. Energy 211 (2020) 1270–1282.
[8] T.I.C.o.N.-I.R. Protection, Guidelines on limits of exposure to ultraviolet radiation of wavelengths between 180 nm and 400 nm (incoherent optical radiation), Health Phys. 87 (2) (2004) 171–186.
[9] J. D`Orazio, S. Jarrett, A. Amaro-Ortiz, T. Scott, UV radiation and the skin, Int. J. Mol. Sci. 14 (6) (2013) 12222–12248.
[10] G. Salvadori, D. Lista, C. Burattini, L. Gugliermetti, F. Leccese, F. Bisegna, Sun exposure of body districts: development and validation of an algorithm to predict the erythemal ultra violet dose, Int. J. Environ. Res. Publ. Health 16 (2019) 3632.
[11] I.C.o.N.-I.R. Protection, ICNIRP guidelines on limits of exposure to incoherent visible and infrared radiation, Health Phys. 105 (1) (2013) 74–96.
[12] A.M. Stoll, Heat transfer in biotechnology, in: J.P. Hartnett, T.F. Irvine (Eds.), Advances in Heat Transfer, Elsevier, 1967, pp. 65–141.
[13] P. Vecchia, M. Hietanen, B.E. Stuck, E. van Deventer, S. Niu, Protecting Workers from Ultraviolet Radiation, 2007.
[14] D.C. Ross, K.R. Diller, An experimental investigation of burn injury in living tissue, J. Heat Tran. 98 (2) (1976) 292–296.
[15] M. Wang, P. Shen, Investigation of indoor asymmetric thermal radiation in Tibet plateau: case study of a typical office building, Buildings 12 (2) (2022) 129.
[16] L. Chen, E. Ng, Outdoor thermal comfort and outdoor activities: a review of research in the past decade, Cities 29 (2) (2012) 118–125.
[17] Y. Xie, T. Huang, J. Li, J. Liu, J. Niu, C.M. Mak, Z. Lin, Evaluation of a multi-nodal thermal regulation model for assessment of outdoor thermal comfort: sensitivity to wind speed and solar radiation, Build. Environ. 132 (2018) 45–56.
[18] C.S. Fong, N. Aghamohammadi, L. Ramakreshnan, N.M. Sulaiman, P. Mohammadi, Holistic recommendations for future outdoor thermal comfort assessment in tropical Southeast Asia: a critical appraisal, Sustain. Cities Soc. 46 (2019), 101428.
[19] E. Ng, V. Cheng, Urban human thermal comfort in hot and humid Hong Kong, Energy Build. 55 (2012) 51–65.
[20] S. Zheng, J.-M. Guldmann, Z. Liu, L. Zhao, Influence of trees on the outdoor thermal environment in subtropical areas: an experimental study in Guangzhou, China, Sustain. Cities Soc. 42 (2018) 482–497.
[21] J. Li, J. Niu, C.M. Mak, T. Huang, Y. Xie, Assessment of outdoor thermal comfort in Hong Kong based on the individual desirability and acceptability of sun and wind conditions, Build. Environ. 145 (2018) 50–61.
[22] C.K.C. Lam, K.K.-L. Lau, Effect of long-term acclimatization on summer thermal comfort in outdoor spaces: a comparative study between Melbourne and Hong Kong, Int. J. Biometeorol. 62 (7) (2018) 1311–1324.
[23] A.P. Gagge, J.A.J. Stolwijk, Y. Nishi, An effective temperature scale based on a simple model of human physiological regulatiry response, Memoir. Facul. Eng. 13 (Suppl) (1972) 21–36. Hokkaido University.
[24] S. Tanabe, K. Kobayashi, J. Nakano, Y. Ozeki, M. Konishi, Evaluation of thermal comfort using combined multi-node thermoregulation (65MN) and radiation models and computational fluid dynamics (CFD), Energy Build. 34 (6) (2002) 637–646.
[25] D. Fiala, G. Havenith, P. Brode, B. Kampmann, G. Jendritzky, UTCI-Fiala multi-node model of human heat transfer and temperature regulation, Int. J. Biometeorol. 56 (3) (2012) 429–441.
[26] K. Nagano, A. Takaki, M. Hirakawa, Y. Tochihara, Effects of ambient temperature steps on thermal comfort requirements, Int. J. Biometeorol. 50 (1) (2005) 33–39.
[27] Y. Zhang, J. Zhang, H. Chen, X. Du, Q. Meng, Effects of step changes of temperature and humidity on human responses of people in hot-humid area of China, Build. Environ. 80 (2014) 174–183.
[28] R.B. Roemer, J.R. Oleson, T.C. Cetas, Oscillatory temperature response to constant power applied to canine muscle, Am. J. Physiol. 249 (2 Pt 2) (1985) R153–R158.
[29] A. Banerjee, A.A. Ogale, C. Das, K. Mitra, C. Subramanian, Temperature distribution in different materials due to short pulse laser irradiation, Heat Tran. Eng. 26 (8) (2005) 41–49.
[30] Y. Shimazaki, A. Yoshida, R. Suzuki, T. Kawabata, D. Imai, S. Kinoshita, Application of human thermal load into unsteady condition for improvement of outdoor thermal comfort, Build. Environ. 46 (8) (2011) 1716–1724.
[31] M. Schweiker, J. Kolarik, M. Dovjak, M. Shukuya, Unsteady-state human-body exergy consumption rate and its relation to subjective assessment of dynamic thermal environments, Energy Build. 116 (2016) 164–180.
[32] P.R. Hoppe, Heat balance modelling, Experientia 49 (9) (1993) 741–746.
[33] J. Li, J. Niu, C.M. Mak, Study of pedestrians' mixed thermal responses when experiencing rapid and simultaneous variations in sun and wind conditions in urban continuums, Sustain. Cities Soc. 87 (2022), 104169.
[34] J. Li, J. Niu, T. Huang, C.M. Mak, Dynamic effects of frequent step changes in outdoor microclimate environments on thermal sensation and dissatisfaction of pedestrian during summer, Sustain. Cities Soc. 79 (2022), 103670.
[35] P.O. Fanger, Thermal Comfort: Analysis and Applications in Environmental Engineering, McGraw-Hill, New York, 1972.
[36] R. de Dear, G. Brager, Developing an adaptive model of thermal comfort and preference, Build. Eng. 1041 (1998) 1–18.
[37] G.S. Brager, R.J. de Dear, Thermal adaptation in the built environment: a literature review, Energy Build. 27 (1) (1998) 83–96.
[38] Y. Zhang, R. Zhao, Relationship between thermal sensation and comfort in non-uniform and dynamic environments, Build. Environ. 44 (7) (2009) 1386–1391.
[39] Y. Ji, J. Song, P. Shen, A review of studies and modelling of solar radiation on human thermal comfort in outdoor environment, Build. Environ. 214 (2022), 108891.
[40] M. La Gennusa, A. Nucara, G. Rizzo, G. Scaccianoce, The calculation of the mean radiant temperature of a subject exposed to the solar radiation—a generalised algorithm, Build. Environ. 40 (3) (2005) 367–375.
[41] H. Zhang, R.Q. Yang, S.J. You, W.D. Zheng, X.J. Zheng, T.Z. Ye, The CPMV index for evaluating indoor thermal comfort in buildings with solar radiation, Build. Environ. 134 (2018) 1–9.
[42] K.J.L. Dusan Fiala, Martin Stohrer, First principles modeling of thermal sensation responses in steady-state and transient conditions, Build. Eng. 109 (1) (2003) 179–186.
[43] Z. H, Human Thermal Sensation and Comfort in Transient and Non-uniform Thermal Environments, University of Carlifornia at Berkeley, Berkeley, 2003. Ph.D. thesis.
[44] J.W. Ring, R. de Dear, Temperature transients: a model for heat diffusion through the skin, thermoreceptor response and thermal sensation, Indoor Air 1 (4) (1991) 448–456.
[45] A. Zolfaghari, M. Maerefat, A new predictive index for evaluating both thermal sensation and thermal response of the human body, Build. Environ. 46 (4) (2011) 855–862.
[46] N.M. Khiavi, M. Maerefat, S.A. Zolfaghari, A new local index for predicting local thermal response of individual body segments, J. Therm. Biol. 78 (2018) 161–173.
[47] A.P. Gagge, A.P. Fobelets, L. Berglund, A Standard Predictive Index of Human Response to the Thermal Environment, 1986.
[48] ASHRAE, ANSI/ASHRAE Standard 55-2017, Thermal Environmental Conditions for Human Occupancy[S], ASHRAE, Atlanta, 2017.
[49] S. Ning, W. Jing, Z. Ge, Sunlight perception and outdoor thermal comfort in college campuses: a new perspective, Sci. Rep. 13 (1) (2023), 16112.
[50] H. Zhang, Human Thermal Sensation and Comfort in Transient and Non-uniform Thermal Environments, 2003.
[51] P.R. Hoppe, The physiological equivalent temperature - a universal index for the biometeorological assessment of the thermal environment, Int. J. Biometeorol. 43 (2) (1999) 71–75.
[52] VDI, Environmental meteorology, Methods for the Human Biometereological Evaluation of Climate and Air Quality for the Urban and Regional Planning at Regional Level, 2008.